Mineralocorticoid Receptor Antagonism by Finerenone Attenuates Established Pulmonary Hypertension in Rats.

Ly Tu, Raphaël Thuillet, Julie Perrot, Mina Ottaviani, Emy Ponsardin, Peter Kolkhof, Marc Humbert, Say Viengchareun, Marc Lombès, Christophe Guignabert

▶ **To cite this version:**

Ly Tu, Raphaël Thuillet, Julie Perrot, Mina Ottaviani, Emy Ponsardin, et al.. Mineralocorticoid Receptor Antagonism by Finerenone Attenuates Established Pulmonary Hypertension in Rats.. Hypertension, 2022, pp.101161HYPERTENSIONAHA12219207. ⟨10.1161/HYPERTENSIONAHA.122.19207⟩. ⟨inserm-03755156⟩

HAL Id: inserm-03755156

https://inserm.hal.science/inserm-03755156v1

Submitted on 22 Aug 2022

HAL is a multi-disciplinary open access archive for the deposit and dissemination of scientific research documents, whether they are published or not. The documents may come from teaching and research institutions in France or abroad, or from public or private research centers.

L'archive ouverte pluridisciplinaire **HAL**, est destinée au dépôt et à la diffusion de documents scientifiques de niveau recherche, publiés ou non, émanant des établissements d'enseignement et de recherche français ou étrangers, des laboratoires publics ou privés.

HAL Authorization

Mineralocorticoid Receptor Antagonism by Finerenone Attenuates Established Pulmonary Hypertension in Rats

Ly Tu [1,2], Raphaël Thuillet [1,2], Julie Perrot [3], Mina Ottaviani [1,2], Emy Ponsardin[4], Peter Kolkhof [5], Marc Humbert [1,2,6], Say Viengchareun [3], Marc Lombès [3,†], and Christophe Guignabert [1,2,†]

[†] Both authors contributed equally to this work

[1] INSERM UMR_S 999 « Pulmonary Hypertension: Pathophysiology and Novel Therapies », Hôpital Marie Lannelongue, 92350 Le Plessis-Robinson, France

[2] Université Paris-Saclay, Faculté de Médecine, 94276 Le Kremlin-Bicêtre, France

[3] Université Paris-Saclay, Inserm, Physiologie et Physiopathologie Endocriniennes, 94276 Le Kremlin-Bicêtre, France

[4] Université Paris-Saclay, Inserm, CNRS, Ingénierie et Plateformes au Service de l'Innovation Thérapeutique, 92296, Châtenay-Malabry, France

[5] BAYER AG, Heart and Vascular Diseases, Therapeutic Area Cardiovascular Diseases, Research and Early Development, Pharmaceuticals, Aprather Weg 18a, 42096 Wuppertal, Germany

[6] Assistance Publique - Hôpitaux de Paris (AP-HP), Service de Pneumologie et Soins Intensifs Respiratoires, Hôpital Bicêtre, 94270 Le Kremlin-Bicêtre, France

Address correspondence to: Christophe Guignabert, Ph.D, INSERM UMR_S 999, 133 Avenue de la Résistance, 92350 Le Plessis-Robinson, France. Phone: +33-1-40842544, Fax: +33-1-40942522, E-mail: *christophe.guignabert@inserm.fr*

ABSTRACT

Aims: We studied the ability of the non-steroidal Mineralocorticoid Receptor (MR) antagonist finerenone to attenuate vascular remodeling and pulmonary hypertension (PH) using two complementary preclinical models [the monocrotaline (MCT) and Sugen/Hypoxia (SuHx) rat models] of severe PH.

Methods and Results: We first demonstrated that MR is overexpressed in experimental and human pulmonary arterial hypertension (PAH) and that its inhibition following siRNA-mediated MR silencing or finerenone treatment attenuates proliferation of pulmonary artery smooth muscle cells (PA-SMCs) derived from idiopathic PAH patients. In addition, we obtained evidence that MR-overexpressing (hMR^{+}) mice display increased right ventricular systolic pressures (RVSP), right ventricular hypertrophy and remodeling of small pulmonary vessels. Consistent with these observations, finerenone (1 mg/kg/day by gavage), started 2 weeks after MCT injection or 5 weeks after Sugen (SU5416) injection, partially reversed established PH, reducing total pulmonary vascular resistance and vascular remodeling. Finally, we also found that continued finerenone treatment decreases inflammatory cell infiltration and vascular cell proliferation in lungs of MCT and SuHx rats.

Conclusion: Finerenone treatment appears to be a potential therapy for PAH worthy of investigation and evaluation for clinical use in conjunction with current PAH treatments.

Keywords: *Pulmonary hypertension, Pulmonary vascular remodeling, Mineralocorticoid receptor, Aldosterone, Finerenone,*

Introduction

Pulmonary arterial hypertension (PAH) is a rare and severe cardiopulmonary condition for which there is no cure at this time, resulting in progressive right heart failure and functional decline[1,2]. A dependable treatment that could directly interfere with specific mechanisms involved in the progression of obstructive pulmonary vascular remodeling to limit the chronic elevation in pulmonary vascular resistance (PVR) is therefore urgently needed. Accumulation of pulmonary artery smooth muscle cells (PA-SMCs) and perivascular inflammatory cell infiltrate are two central mechanisms in this process[2-4], but the exact underlying mechanisms remain unknown.

Evidence suggests that Mineralocorticoid Receptor (MR), a steroid hormone receptor belonging to the nuclear receptor superfamily of transcription factors, could be targeted in PAH to limit pulmonary vascular cell accumulation[5-9]. The dysfunctional pulmonary endothelium is indeed a local source of the classical MR ligand aldosterone in remodeled vessels of PAH patients[10], which through MR activation, may facilitate SMC proliferation, inflammation and oxidative stress[5,6,10-19]. In addition, MR can be activated by a direct and rapid action of oxidative stress and/or angiotensin (Ang)II, through AT1 receptor binding in a non-classical pathway[15-17]. Since, in PAH, there is also a local overproduction of endothelial-derived AngII associated with the AT1 overexpression in PA-SMCs[20], we hypothesized that a local over-activation of MR signaling in resident vascular cells or/and in perivascular immune cells may play an important role in the pathogenesis of PAH. Consistent with this notion, both spironolactone, which is a non-selective steroidal MR antagonist (MRA), and eplerenone, a selective steroidal MRA, have been reported to reduce vascular and cardiac remodeling in monocrotaline (MCT) and chronic hypoxia (CHx) models of pulmonary hypertension (PH)[10-14,21].

Finerenone is a first-in-class nonsteroidal MRA that has a higher selectivity and stronger affinity for MR than steroidal MRAs in preclinical models[22,23]. Although chronic treatments with finerenone have anti-inflammatory, anti-fibrotic, and anti-proliferative properties in several *in vivo* experimental models[24-27], its efficacy in rat models of severe PH has not been studied yet. The purpose of this study was to determine the potential benefit of chronic treatments with finerenone in two complementary preclinical models [the monocrotaline (MCT) and Sugen/Hypoxia (SuHx) rat models] of severe PH.

Methods

Animal models of severe PH and *in vivo* treatment

Four-week-old male Wistar rats weighing 100 g (Janvier Labs, Saint Berthevin, France) were studied 3 weeks after a single subcutaneous injection of MCT (60 mg/kg; Sigma-Aldrich, Saint-Quentin-Fallavier, France) or vehicle[28]. Male rats were used to minimize hormonal effects. At day-14, MCT-injected rats were randomly divided into two groups and treated for 2 weeks with daily *per os* treatment with either vehicle [ethanol:PEG400:water, 10:40:50%] or finerenone in vehicle (1 mg/kg/day, Bayer AG, Wuppertal, Germany). Two additional groups of age-matched control rats were constituted and treated for 2 weeks with daily *per os* treatment with vehicle or finerenone. To further strengthen the findings obtained in the MCT rat model, a second rat model of severe PH was used. Briefly, 16 male Wistar rats (100 g, Janvier Labs) received a single subcutaneous injection of SU5416 (20 mg/kg) and were exposed to normobaric hypoxia for 3 weeks before to return to room air for 5 weeks. At 5-weeks post-SU5416 injection, pulsed-wave doppler during transthoracic echocardiography was used to validate the presence of established PH by assessing pulmonary artery acceleration time (AT)/ ejection time (ET) ratio, using Vivid E9 (GE Healthcare, Velizy-Villacoublay, France). Then, SuHx rats were randomized to receive vehicle or finerenone (1 mg/kg/day).

Echocardiography and right ventricle (RV) hemodynamic measurements

Rats were anesthetized *via* inhaled isoflurane at 2.0% in room air and body temperature was maintained at 37°C. Transthoracic echocardiography was used to blindly determine AT/ET. Then, pulmonary pressures were measured blindly by closed chest right heart catheterization, as previously described. Briefly, a polyvinyl catheter was introduced into the right jugular vein and pushed through the RV into the pulmonary artery. In parallel, a carotid artery was cannulated for the measurement of systemic arterial pressure. Cardiac output (CO) in rats was measured using the thermodilution method. Hemodynamic values were automatically calculated by the physiological data acquisition system (LabChart 7 Software; ADInstruments Co., Shanghai, China). After measurement of hemodynamic parameters, the thorax was opened and the left lung immediately removed and frozen. The right lung

was fixed in the distended state with formalin buffer. The heart was then removed, and the RV wall, LV wall, and interventricular septum (S) were dissected and weighed, and the ratio of RV to LV plus S weight [RV/(LV+S)] was calculated as the Fulton index to assess RV hypertrophy. The percentage of wall thickness [(2 × medial wall thickness/ external diameter) × 100] and of muscularized vessels were performed as previously described[28].

Transgenic mice overexpressing MR

To generate MR-overexpressing mice (*hMR*$^{+}$ mice), the human *MR* gene was placed under the control of the proximal P1 promoter into the B6D2F1 mouse strain as previously described[29]. The offspring genotypes were determined by PCR and we confirmed that the mice are viable and fertile, and have a normal life span and growth rate.

Mice were studied in room air at approximately 12 weeks of age. For echocardiography, mice were anesthetized under gaseous anaesthesia (Isoflurane-Vetflurane, Virbac 1.8-2% in a 1:1 mixture of oxygen:air). Hairs of the thoracic area were removed (hair-removing cream for sensitive skin), and the animal was positioned on a heating platform linked to the echography system (Vevo® 3100 LT, Fujifilm VisualSonics Inc., Toronto, Canada) allowing the registration of ECG and respiratory rate. MS-550D (55 MHz) transducer was used for image acquisition and determination of AT:ET ratio and CO; this transducer is specifically dedicated to mouse cardiac imaging (VisualSonics). As previously described [30], hemodynamic parameters were measured in unventilated anesthetized mice *via* inhaled isoflurane at 2.0% in room air using a closed chest technique by introducing a 1.4-F Millar catheter (ADInstruments, Paris, France) into the jugular vein and directing it to the RV to assess the right ventricular systolic pressure (RVSP). After the hemodynamic assessments were completed, the heart and lungs were then removed *en bloc* to assess RV and pulmonary vascular changes.

Isolation, culture, and functional analyses of PA-SMCs from idiopathic PAH patients

Primary cultures of pulmonary artery smooth muscle cells (PA-SMCs) from idiopathic PAH patients were isolated using an explant-outgrowth method and cultured as previously described[31-34]. Briefly, small pieces of freshly micro-dissected pulmonary arteries were cultured in Dulbecco modified Eagle

medium supplemented with 15% fetal calf serum (FCS), 2 mM L-glutamine, and antibiotics (100 unit/ml penicillin and 100 µg/ml streptomycin). The isolated pulmonary PA-SMCs were strongly positive for α-smooth muscle actin, smooth muscle–specific SM22 protein, and calponin, and negative for von Willebrand factor and CD31. PA-SMCs were routinely tested for mycoplasma and used at early passages < 7. To knockdown MR expression, PA-SMCs were transfected with 100 nM of MR siRNA or with scrambled sequence (Horizon Discovery, Cambridge, UK) using lipofectamine RNAiMAX according to the manufacturer's recommendations. To assess cell proliferation, PA-SMCs were seeded in 96-well plates at a density of 3,000 cells/well and allowed to adhere. After being subjected to growth arrest for 48 h in medium lacking FCS, the PA-SMCs were treated with vehicle or finerenone in presence of 5% FCS. Then, PA-SMC proliferation was assessed by measuring 5-bromo-2-deoxyuridine incorporation using a DELFIA kit (Perkin Elmer, Villebon-Sur-Yvette) as recommended by the manufacturer. BrdU incorporation was determined by measuring Eu-fluorescence in a time-resolved EnVision Multilabel Reader (PerkinElmer, Waltham, MA, USA).

RNA purification and RNA sequencing data analysis

Total RNA quality was assessed on an Agilent Bioanalyzer 2100, using RNA 6000 pico kit (Agilent Technologies). Directional RNA-Seq Libraries were constructed using the TruSeq Stranded Total RNA library prep kit (Illumina), following the manufacturer's instructions, 1 µg of total RNA was used. After Ribo-Zero depletion, the samples were checked on the Agilent Bioanalyzer for proper rRNA depletion. Final library quality was assessed on an Agilent Bioanalyzer 2100, using an Agilent High Sensitivity DNA Kit. Libraries were pooled in equimolar proportions and sequenced on three paired-end 42bp runs, on an Illumina NextSeq500 instrument, using NextSeq 500 High Output 75 cycles kits. Demultiplexing has been done (bcl2fastq2 V2.15.0) and adapters removed (Cutadapt1.3), only reads longer than 10pb were kept for analysis. All data analysis were performed using R and RStudio software. Reads were independently mapped to the human genome GRCh38 using Rsubread package[35]. Read count was generated with Rsubread using ensembl GTF file release-105 at gene level. Genes with read count mean lower than 1 were discarded for downstream analyses. TMM normalization was done using edgeR package[36] and normalized data were linearized with voom

function from Limma R package[37]. To find differentially expressed genes, we applied a two-way analysis of variance for treatment and batch effect for each gene and made pairwise Tukey's post hoc tests between groups. We then considered as significant genes with p-value < 0.01 and fold-change > 1.5 for upregulation and fold-change < -1.5 for downregulation. For functional enrichment analysis we used MSigDB v7.5 as geneset database and applied Fisher exact test with FDR correction p-value for multiple testing. All raw and processed data have been submitted on GEO NCBI database with the accession number GSE202698.

Western blot and immunostaining

Tissues were homogenized and sonicated in RIPA buffer containing protease and phosphatase inhibitors (Sigma Aldrich). From 20 to 50 µg of protein was used to detect MR and β-actin as previously described[38]. For *in situ* studies, we used lung specimens obtained after lung transplantation of patients with idiopathic PAH and lobectomy or pneumonectomy for localized lung cancer of control subjects. Preoperative echocardiological evaluations, including echocardiography, were performed on the control subjects to rule out PAH and the lung specimens from the control subjects were collected distant from the tumor foci. The absence of tumoral infiltration was retrospectively established for all tissue sections by histopathological analysis. Immunohistochemistry or immunocytofluorescent staining for MR (39N antibody[39,40]), alpha-smooth muscle actin (α-SMA, Santa Cruz Biotechnology), CD68 (Santa Cruz Biotechnology, Heidelberg, Germany), and proliferating cell nuclear antigen (PCNA, Dako, Les Ulis, France) and KI67 (Zytomed Systems, Berlin, Germany) were performed in human or rodent lung paraffin sections. Briefly, 5-µm thick lung sections were deparaffinized and stained with Hematoxylin and Eosin, Sirius red (Sigma-Aldrich), or incubated with retrieval buffer. Then, sections were saturated with blocking buffer and incubated overnight with specific antibodies, followed by incubation with the appropriate dilution of the corresponding secondary fluorescently labeled antibodies (ThermoFisher Scientific, Illkirch, France). Nuclei were labeled using DAPI (ThermoFisher Scientific). Mounting was performed using ProLong Gold antifade reagent (ThermoFisher Scientific). The images were captured using an LSM700 confocal microscope (Zeiss, Marly Le Roi, France) with ZEN software. Other lung sections were used for immunochemistry using

vectastain ABC kit according to the manufacturer's instructions (Abcys, Courtaboeuf, France) and counterstained with Hematoxylin (Sigma-Aldrich). Images were taken using Eclipse 80i microscope (Nikon Instruments, Champigny-sur-Marne, France).

Statistical Analyses

The data are expressed as the means±SEM. Mann-Whitney *U*-tests were used to assess the statistical significance of differences between two groups. Comparisons concerning more than two groups were calculated by ANOVA, followed by the Tukey test for data with a normal distribution. Differences were considered significant for $P<0.05$. Analyses were performed using PRISM software (GraphPad, la Jolla, CA, USA, version 7).

Ethics statement

Animal experiments were approved by the Ethics Committee of the Université Paris-Saclay and carried out in accordance with the Guide for the Care and Use of Laboratory Animals adopted by the National Institute of Health and Medical Research (Inserm). The use of human tissue was approved by the local ethics committee (CPP EST-III n°18.06.06, Le Kremlin-Bicêtre, France) and all patients gave informed consent before the study.

Results

MR is overexpressed in remodeled PAs in lungs of idiopathic PAH patients, MCT and SuHx rats

Confocal microscopic analyses and double labeling for MR and α-SMA were used to determine and compare MR protein expression patterns in lung specimens from control subjects and patients with idiopathic PAH as well as in lungs of control, MCT and SuHx rats. In control human lung tissues, we found that MR is expressed at low levels in different cell types of the pulmonary arterial wall of remodeled pulmonary arteries including in PA-SMCs, endothelial cells and different cells present in the adventitia. However, PAH lung specimens displayed a more pronounced staining for MR relative

to control lung tissues. This MR overexpression was independent of vessel diameter (**Figure 1A**). Our data indicate a 3-fold increase in the relative fluorescence mean intensity (FMI) of the MR signals in the smooth muscle (FMI=44±19 *v* 13±5; *P=0.01*, respectively) and in PA-SMC nuclei (FMI=66±17 *vs.* 22±6; *P=0.04*, respectively) between idiopathic PAH and controls. In sharp contrast, no difference was found in the relative FMI of the MR signals in the endothelial layer (FMI=36±14 *vs* 22±9; *P=0.41*, respectively) and EC nuclei (FMI=68±19 *vs* 40±12; *P=0.41*, respectively) between lungs from idiopathic PAH and controls.

These observations were replicated in two different animal models of severe PH, with a more pronounced MR staining in PA-SMCs of remodeled vessels in MCT- and SuHx-rat lungs (FMI=15.4±7.1 *vs* 9.9±3.5; *P=0.05,* and 37.4±4.1 *vs* 13.1±0.6; *P=0.001* between MCT or SuHx *vs* control rat lungs, respectively) (**Figure 1B**). Consistent with the *in situ* data, the mean mRNA and protein levels of MR were increased in cultured PA-SMCs derived from idiopathic PAH patients, relative to controls (**Supplemental Fig. S1**). In contrast, no difference in MR protein levels were found between cultured pulmonary microvascular endothelial cells derived from idiopathic PAH patients and controls (0.94±0.16 *vs* 0.59±0.94; *NS, respectively*).

MR inhibition following siRNA-mediated MR silencing or finerenone treatment attenuates proliferation of PAH PA-SMCs

To obtain a global view of the role of MR in human PA-SMCs, comparative transcriptome analyses between PA-SMCs transfected with either a MR siRNA or a scrambled sequence were performed in our study **(Figure 2A-C and Supplemental Fig. S2)**. Transfecting PAH PA-SMCs with MR siRNA decreased the MR protein level by more than 50% compared with scrambled sequence. A total of 908 differentially expressed genes (DEGs) including 536 upregulated genes and 372 downregulated genes were detected in PAH PA-SMCs transfected with MR-siRNA as compared with PAH PA-SMCs transfected with Src Seq (**Figure 2A**). The gene ontology (GO) analysis of DEGs with significant differences revealed that they are involved in critical biological processes and molecular pathways, such as mitotic cell cycle, microtubule-based process, macromolecule catabolic process,

organonitrogen compound catabolic process, intracellular transport, and cell cycle (**Figure 2B and Supplemental Fig. S3**). The analysis of enriched KEGG and Reactome pathways also confirmed the association of the DEGs in cell cycle mitotic, cell cycle, and DNA replication (**Figure 2B and Supplemental Fig. S3**). The volcano plot (**Figure 2C**) showed global expression changes in MR knockdown PA-SMCs. Taken together, these RNAseq data suggest that knocking out MR expression slowed down PA-SMC proliferation *in vitro*.

Subsequent studies were carried out to confirm the association between MR activation and PCNA staining in lung specimens from control subjects and patients with idiopathic PAH using confocal microscopic analyses and double labeling for MR and PCNA. Positive staining of both MR and PCNA were noted in vascular cells in remodeled PAs in lungs of idiopathic PAH patients (**Figure 2D**). Since our data indicate that cultured PA-SMCs derived from PAH patients at early passages (< 7) maintained *in vitro* their MR overexpression (**Supplemental Figure S1**), we next explored the effect of MR inhibition on the abnormal proliferation of PA-SMCs derived from idiopathic PAH patients. Compared with scrambled sequence, MR siRNA decreased the proliferation of PAH PA-SMCs induced by 5% FCS (**Figure 2E**) and reduced expression of several genes found to be regulated by MR and involved in cell proliferation and cell cycle control, such as *CCND1*, *CDC45*, *ESPL1*, *FZR1*, *MCM5*, and *PLK1* (**Supplemental Fig. S2 and Figure 2C).** Consistent with these findings, finerenone (10^{-6} M) also reduced PAH PA-SMCs proliferation compared to vehicle (**Figure 2F**). Taken together, these results support the notion that MR contributes to the PH-associated pulmonary vascular remodeling.

Increased pulmonary vascular resistance and remodeling of pulmonary vessels in transgenic mice overexpressing MR (hMR^+)

Next, to better understand the functional importance of MR activation in the pulmonary vascular remodeling characteristic of PH, we used hMR^+ mice in which the *hMR* gene is ubiquitously overexpressed (**Supplemental Fig S4**). Doppler-echocardiographic assessment of the left ventricular (LV) structure and function was first performed in anesthetized adult WT and hMR^+ mice and no significant changes in the cardiac output (CO) and AT/ET were found (**Figure 3A**). Invasive

hemodynamic using right heart catheterization confirmed the presence of mild PH in hMR^+ mice as reflected by a significant elevation in the values of right ventricular systolic pressure (RVSP) (P<0.05) and Fulton index [RV/(LV+S)] (P<0.05), indicators of right ventricular hypertrophy (**Figure 3B**), and the percentage of medial thickness and muscularized pulmonary arteries (**Figure 3C**). Consistent with our previous study indicating that hMR^+ mice do not display changes in mean arterial blood pressure[29], no difference in left ventricle (LV)+ Septum (S) mass was observed between hMR^+ and WT mice (101.8±5.2 *vs* 104.2±4.7; NS, respectively). Finally, we found that in association with the increased expression of cyclin D1 in hMR^+ mouse lungs (**Supplemental Fig S4**), the number of positive cells for the cell proliferation antigen KI67 in remodeled pulmonary vessels from hMR^+ mice and the number of perivascular CD68-positive cells (macrophages) were significantly higher than in WT mouse lungs (**Figure 3D**), supporting the notion that MR activation confers PH and increased pulmonary vascular remodeling in mice.

Chronic treatment with finerenone partially reverses PH in the monocrotaline (MCT) and sugen+hypoxia (SuHx) rats

Based upon these findings, we next tested the effect of chronic finerenone treatment against the progression of PH induced in rats by MCT or SuHx. No rats died during these studies. Compared with control rats, a substantial decrease in the ratios of AT/ET were found in vehicle-treated MCT rats 4 weeks post-MCT injection, without changes of systemic blood pressure. However, this reduction was less pronounced in rats chronically treated with finerenone (**Figure 4A-C**). Consistent with these echocardiographic data, invasive hemodynamic measurements using right heart catheterization confirmed the presence of PH in vehicle-treated MCT rats as reflected by the increase in mean pulmonary artery pressure (mPAP), total pulmonary vascular resistance (TPVR) and RV/(RV+LV) ratio, together with a decrease in CO (**Figure 4D**). Importantly, finerenone treatment partially reversed established PH in MCT rats, reducing total pulmonary vascular resistance and right ventricular hypertrophy. Consistent with our observations in the MCT rat model, we confirmed that curative finerenone treatment also partially reverses PH in a second experimental model of severe PH, namely the SuHx rat model (**Figure 4E**). Before treatment (week-5), transthoracic echocardiography validated

that SuHx rats exhibit established PH, as reflected by lower values of AT/ET ratio (**Figure 4F**). Compared with control rats, vehicle- and finerenone-treated rats exhibited lower AT/ET ratios 8 weeks post-SU5416 injection, but this reduction was less pronounced in finerenone-treated SuHx rats compared to vehicle-treated rats, suggesting protective effect of finerenone treatment against the pulmonary vascular remodeling induced by SuHx (**Figure 4F**). There were no significant differences in mean blood pressure between groups (**Figure 4G**). In addition, we found that values of mPAP, TPVR and RV/(RV+LV) ratio were reduced in finerenone-treated SuHx rats than in vehicle-treated SuHx rats. Furthermore, we observed that finerenone-treated SuHx rats exhibit an improved cardiac output (**Figure 4H**).

Consistent with these results, vehicle-treated MCT and SuHx rats exhibited an increase in the accumulation of collagen (stained with picosirius red) in the RV **(Figure 5A)** as well as in the percentages of medial wall thickness and of muscularized distal pulmonary arteries **(Figure 5B)**. In contrast, our results indicated that finerenone-treated MCT and SuHx rats display a reduced accumulation of collagen in the RV and lower percentages of medial wall thickness and of muscularized distal pulmonary arteries relative to vehicle-treated MCT and SuHx rats (**Figure 5**). We next showed that chronic treatment with finerenone decreases inflammatory cell infiltration (CD68 staining) and vascular cell proliferation (KI67 staining) in lung of MCT and SuHx rats (**Figure 6**).

Taken together, our results indicate that chronic treatment with finerenone partially attenuates PA-SMCs proliferation and decreases inflammatory cell infiltration in these two different animal models of severe PH.

Discussion

Although finerenone has anti-inflammatory, anti-fibrotic, and anti-proliferative properties in several *in vivo* experimental models[24-27], its efficacy in rat models of severe PH has never been studied. Herein, we obtained evidence indicating that MR contributes to the aberrant cell accumulation within the pulmonary vasculature in human and experimental PAH. We first showed that MR is overexpressed in

PAH remodeled vessels relative to control subjects and that its inhibition following siRNA-mediated MR silencing or finerenone treatment attenuates the proliferation of PA-SMCs derived from patients with idiopathic PAH. We also demonstrated that transgenic mice that overexpress MR (*hMR*$^+$ mice) present increased right ventricular systolic pressures, right ventricular hypertrophy, and remodeling of small pulmonary vessels and a 2-fold increase in the percentage of PCNA-positive pulmonary vascular cells compared with their wild-type littermates. Finally, we also demonstrated that chronic treatment with finerenone at a dose which does not modify systemic blood pressure, partially attenuates PA-SMC proliferation and inflammatory cell infiltration in lungs of MCT and SuHx rats with established PH.

Elevated plasma and lung tissue levels of the two MR activators aldosterone and Ang-II are found in patients with idiopathic PAH[8,20], suggesting that MR may be overactivated in lungs of PAH patients. Our study provides direct experimental evidence that MR is overexpressed in PA-SMCs of remodeled pulmonary arteries in patients with idiopathic PAH as well as in MCT and SuHx rats with established PH. Since MR is known to promote vascular oxidative stress, inflammation, proliferation, migration, vasoconstriction, vascular remodeling, and fibrosis and because circulating aldosterone and Ang-II levels have been reported to correlate with the disease severity[7,10,20], MR may play a pivotal role in PAH pathogenesis. To support this hypothesis, we performed Doppler-echocardiographic assessment of the left ventricular (LV) structure and function in anesthetized adult WT and *hMR*$^+$ mice and showed that *hMR*$^+$ mice exhibit mild pulmonary vascular remodeling and right ventricular hypertrophy in room air.

Several preclinical studies have demonstrated that MR antagonism with either spironolactone (first generation) or eplerenone (second generation) have beneficial effects in the chronic hypoxia-induced PH with or without administration of the VEGFRII inhibitor SU5416[11,12] as well as in the MCT and SuHx rat models of severe PH[10,13]. However, it is well known that clinical use of these two steroidal MRAs presents several disadvantages. Unselective binding of spironolactone to the androgen receptor as an antagonist and to the progesterone receptor as an agonist is responsible for sexual adverse effects including gynecomastia and impotence[41]. Eplerenone is much more selective than spironolactone but has a relatively low *in vitro* affinity for the MR. Importantly, the use of both

steroidal antagonists is associated with the risk of developing life-threatening hyperkalemia and worsening of renal function[41]. Recently, the non-steroidal third generation of MRA finerenone, a potent and highly selective MRA has been developed[22-26]. Furthermore, addition of finerenone to optimal renin-angiotensin system (RAS) blockade reduced cardiovascular (CV) and kidney outcomes in two large phase III trials in patients with chronic kidney disease (CKD) and type 2 diabetes (T2D)[42,43]. The incidence of hyperkalemia-related discontinuation (2.3% vs. 0.9% in placebo) was markedly lower than with spironolactone on top of RAS blockade in CKD patients[43]. In contrast to the other MR antagonists, finerenone has been reported to act as an inverse MR agonist preventing the recruitment of key transcriptional cofactors on the promoter of the different MR target genes[25,44]. Herein, we obtained evidence that MR inhibition following siRNA-mediated MR silencing or finerenone treatment attenuates the proliferation of PA-SMCs derived from patients with idiopathic PAH and partially reverses experimental PH in the MCT and SuHx rat models of severe PH.

The molecular mechanism underlying the protective effects of finerenone against the pulmonary vascular remodeling in the MCT and SuHx rats remains unknown, however our findings indicate that it may partly be mediated by a decrease in PA-SMC proliferation and a reduction of inflammatory cell infiltration in lungs of finerenone-treated MCT and SuHx rats. These data are consistent with the recent study from Menon and colleagues[21], which showed that the degree of perivascular lung inflammation is higher in mice with a smooth muscle-specific deletion of MR when they are subjected to SU5416 in combination with chronic hypoxia. Consistent with these results, we also found a significant increase in the percentage of KI67-positive pulmonary vascular cells and a perivascular accumulation of CD68-positive cells in lungs of *hMR*$^{+}$ mice. As underlined by other studies, MR is a pleiotropic factor with central roles in endothelial or immune cell responses, therefore we cannot exclude that finerenone exerts also protective effects through the modulation of the endothelial-[12,13] and/or macrophage-MR signaling[45,46]. Using genetically modified mouse models with tissue-specific MR deletion, Kowalski *et al*. have indeed recently demonstrated that only mice with deletion of the *MR* gene in endothelial cells, but not in SMCs, fibroblasts, or in myeloid cells, are less prone to remodel pulmonary vessels under chronic hypoxia than wild-type mice[12]. However, Menon *et al.*[21] recently reported that endothelial MR deletion was not sufficient to protect mice exposed to chronic

hypoxia combined with SU5416 injection. However, these two different studies found beneficial effects of MR inhibition by eplerenone[12] and spironolactone[21] in these mouse models of experimental PH, respectively. Taken altogether, these studies reveal cell-type specific roles of MR in the context of PAH that is consistent with the decrease in PA-SMC proliferation and the reduction of inflammatory cell infiltration observed in lungs of finerenone-treated MCT and SuHx rats. Therefore, further studies are needed to study whether finerenone could attenuate abnormal phenotypic features of pulmonary endothelial cells found in idiopathic PAH.

In summary, these findings underline that MR contributes to the aberrant cell accumulation within the pulmonary vasculature in human and experimental PAH. Our data also demonstrate that finerenone treatment attenuates pulmonary vascular remodeling and decreases pulmonary arterial pressure in two different experimental models of severe PH. Our data indicate that this beneficial effect is mediated not only by a decrease in PA-SMCs proliferation, but also by reduction of inflammatory cell infiltration in lungs of finerenone-treated MCT and SuHx rats. Our findings should encourage clinical investigations and especially the evaluation of the use of finerenone in conjunction with current PAH therapies.

Acknowledgments: The authors thank Jérôme Fagart, Florian Le Billan, Damien Le Menuet, Alice Huertas, Florent Dumont, and Larbi Amazit for their support and assistance. We also acknowledge the sequencing and bioinformatics expertise of the I2BC High-throughput sequencing facility, supported by France Génomique (funded by the French National Program "Investissement d'Avenir" ANR-10-INBS-09). The authors thank Vincent Thomas de Montpreville and his team from the Pathology Department/ Centre de Recherche Biologique at Marie Lannelongue Hospital - Groupe Hospitalier Paris Saint Joseph for their expertise and support. They also thank all participants of the French PH Network PulmoTension.

Support statement: This research was supported by grants from the French National Institute for Health and Medical Research (Inserm), the Paris-Saclay University, the Marie Lannelongue Hospital, the French National Agency for Research (ANR) grant n° ANR-16-CE17-0014 (TAMIRAH), and in part by the Département Hospitalo-Universitaire (DHU) Thorax Innovation (TORINO), the Assistance Publique-Hôpitaux de Paris (AP-HP), Service de Pneumologie, Centre de Référence de l'Hypertension Pulmonaire Sévère, the French PAH patient association (HTAP France), and the Fondation du Souffle (FdS).

Authors Contributions: Conception and design: LT, SV, ML and CG; Analysis and interpretation: all; Drafting manuscript: LT, SV, ML and CG. All authors read and corrected the manuscript and approved the final manuscript.

Abbreviations: *α-smooth muscle actin:* ***α-SMA****; acceleration time:* ***AT****; arbitrary unit:* ***AU****; blood pressure:* ***BP****; bone morphogenetic protein receptor type II:* ***BMPRII****; 5-bromo-2'-deoxyuridine:* ***BrdU****; cardiac output:* ***CO****; ejection time:* ***ET****; fetal calf serum:* ***FCS****; left ventricle:* ***LV****; mean pulmonary arterial pressure:* ***mPAP****; monocrotaline:* ***MCT****; mineralocorticoid receptor :* ***MR****; pulmonary arteries:* ***PAs****; pulmonary arterial hypertension:* ***PAH****; pulmonary artery-smooth muscle cell:* ***PA-SMC****; proliferating cell nuclear antigen* ***PCNA****; right ventricle:* ***RV****; right ventricular systolic pressure:* ***RVSP****; septum:* ***S****; SU5416 combined with hypoxia:* ***SuHx****; total pulmonary vascular resistance:* ***TPVR****; wild-type:* ***WT****.*

REFERENCES:

1. Simonneau G, Gatzoulis MA, Adatia I, Celermajer D, Denton C, Ghofrani A, Gomez Sanchez MA, Krishna Kumar R, Landzberg M, Machado RF, et al. Updated clinical classification of pulmonary hypertension. *Journal of the American College of Cardiology*. 2013;62:D34-41. doi: 10.1016/j.jacc.2013.10.029

2. Humbert M, Guignabert C, Bonnet S, Dorfmuller P, Klinger JR, Nicolls MR, Olschewski AJ, Pullamsetti SS, Schermuly RT, Stenmark KR, et al. Pathology and pathobiology of pulmonary hypertension: state of the art and research perspectives. *Eur Respir J*. 2019;53. doi: 10.1183/13993003.01887-2018

3. Huertas A, Tu L, Humbert M, Guignabert C. Chronic inflammation within the vascular wall in pulmonary arterial hypertension: more than a spectator. *Cardiovasc Res*. 2020;116:885-893. doi: 10.1093/cvr/cvz308

4. Lechartier B, Berrebeh N, Huertas A, Humbert M, Guignabert C, Tu L. Phenotypic Diversity of Vascular Smooth Muscle Cells in Pulmonary Arterial Hypertension: Implications for Therapy. *Chest*. 2021. doi: 10.1016/j.chest.2021.08.040

5. Kolkhof P, Barfacker L. 30 YEARS OF THE MINERALOCORTICOID RECEPTOR: Mineralocorticoid receptor antagonists: 60 years of research and development. *J Endocrinol*. 2017;234:T125-T140. doi: 10.1530/JOE-16-0600

6. Giagnorio R, Hansmann G. Mineralocorticoid receptor blockade improves pulmonary hypertension and right ventricular function in bronchopulmonary dysplasia: a case report. *Cardiovasc Diagn Ther*. 2020;10:1686-1690. doi: 10.21037/cdt.2020.02.05

7. Safdar Z, Frost A, Basant A, Deswal A, O'Brian Smith E, Entman M. Spironolactone in pulmonary arterial hypertension: results of a cross-over study. *Pulmonary circulation*. 2020;10:2045894019898030. doi: 10.1177/2045894019898030

8. Maron BA, Waxman AB, Opotowsky AR, Gillies H, Blair C, Aghamohammadzadeh R, Loscalzo J, Leopold JA. Effectiveness of spironolactone plus ambrisentan for treatment of pulmonary arterial hypertension (from the [ARIES] study 1 and 2 trials). *Am J Cardiol*. 2013;112:720-725. doi: 10.1016/j.amjcard.2013.04.051

9. Calvier L, Legchenko E, Grimm L, Sallmon H, Hatch A, Plouffe BD, Schroeder C, Bauersachs J, Murthy SK, Hansmann G. Galectin-3 and aldosterone as potential tandem biomarkers in pulmonary arterial hypertension. *Heart*. 2016;102:390-396. doi: 10.1136/heartjnl-2015-308365

10. Maron BA, Zhang YY, White K, Chan SY, Handy DE, Mahoney CE, Loscalzo J, Leopold JA. Aldosterone inactivates the endothelin-B receptor via a cysteinyl thiol redox switch to decrease pulmonary endothelial nitric oxide levels and modulate pulmonary arterial hypertension. *Circulation*. 2012;126:963-974. doi: 10.1161/CIRCULATIONAHA.112.094722

11. Boehm M, Arnold N, Braithwaite A, Pickworth J, Lu C, Novoyatleva T, Kiely DG, Grimminger F, Ghofrani HA, Weissmann N, et al. Eplerenone attenuates pathological pulmonary vascular rather than right ventricular remodeling in pulmonary arterial hypertension. *BMC Pulm Med*. 2018;18:41. doi: 10.1186/s12890-018-0604-x

12. Kowalski J, Deng L, Suennen C, Koca D, Meral D, Bode C, Hein L, Lother A. Eplerenone Improves Pulmonary Vascular Remodeling and Hypertension by Inhibition of the

Mineralocorticoid Receptor in Endothelial Cells. *Hypertension*. 2021;78:456-465. doi: 10.1161/HYPERTENSIONAHA.120.16196

13. Preston IR, Sagliani KD, Warburton RR, Hill NS, Fanburg BL, Jaffe IZ. Mineralocorticoid receptor antagonism attenuates experimental pulmonary hypertension. *American journal of physiology Lung cellular and molecular physiology*. 2013;304:L678-688. doi: 10.1152/ajplung.00300.2012

14. Yamanaka R, Otsuka F, Nakamura K, Yamashita M, Otani H, Takeda M, Matsumoto Y, Kusano KF, Ito H, Makino H. Involvement of the bone morphogenetic protein system in endothelin- and aldosterone-induced cell proliferation of pulmonary arterial smooth muscle cells isolated from human patients with pulmonary arterial hypertension. *Hypertens Res*. 2010;33:435-445. doi: 10.1038/hr.2010.16

15. Briet M, Barhoumi T, Mian MOR, Coelho SC, Ouerd S, Rautureau Y, Coffman TM, Paradis P, Schiffrin EL. Aldosterone-Induced Vascular Remodeling and Endothelial Dysfunction Require Functional Angiotensin Type 1a Receptors. *Hypertension*. 2016;67:897-905. doi: 10.1161/HYPERTENSIONAHA.115.07074

16. Lu Q, Davel AP, McGraw AP, Rao SP, Newfell BG, Jaffe IZ. PKCdelta Mediates Mineralocorticoid Receptor Activation by Angiotensin II to Modulate Smooth Muscle Cell Function. *Endocrinology*. 2019;160:2101-2114. doi: 10.1210/en.2019-00258

17. Min LJ, Mogi M, Li JM, Iwanami J, Iwai M, Horiuchi M. Aldosterone and angiotensin II synergistically induce mitogenic response in vascular smooth muscle cells. *Circulation research*. 2005;97:434-442. doi: 10.1161/01.RES.0000180753.63183.95

18. Xiao F, Puddefoot JR, Barker S, Vinson GP. Mechanism for aldosterone potentiation of angiotensin II-stimulated rat arterial smooth muscle cell proliferation. *Hypertension*. 2004;44:340-345. doi: 10.1161/01.HYP.0000140771.21243.ed

19. Ishizawa K, Izawa Y, Ito H, Miki C, Miyata K, Fujita Y, Kanematsu Y, Tsuchiya K, Tamaki T, Nishiyama A, et al. Aldosterone stimulates vascular smooth muscle cell proliferation via big mitogen-activated protein kinase 1 activation. *Hypertension*. 2005;46:1046-1052. doi: 10.1161/01.HYP.0000172622.51973.f5

20. de Man FS, Tu L, Handoko ML, Rain S, Ruiter G, Francois C, Schalij I, Dorfmuller P, Simonneau G, Fadel E, et al. Dysregulated renin-angiotensin-aldosterone system contributes to pulmonary arterial hypertension. *Am J Respir Crit Care Med*. 2012;186:780-789. doi: 10.1164/rccm.201203-0411OC

21. Menon DP, Qi G, Kim SK, Moss ME, Penumatsa KC, Warburton RR, Toksoz D, Wilson J, Hill NS, Jaffe IZ, et al. Vascular cell-specific roles of mineralocorticoid receptors in pulmonary hypertension. *Pulm Circ*. 2021;11:20458940211025240. doi: 10.1177/20458940211025240

22. Barfacker L, Kuhl A, Hillisch A, Grosser R, Figueroa-Perez S, Heckroth H, Nitsche A, Erguden JK, Gielen-Haertwig H, Schlemmer KH, et al. Discovery of BAY 94-8862: a nonsteroidal antagonist of the mineralocorticoid receptor for the treatment of cardiorenal diseases. *ChemMedChem*. 2012;7:1385-1403. doi: 10.1002/cmdc.201200081

23. Pitt B, Filippatos G, Gheorghiade M, Kober L, Krum H, Ponikowski P, Nowack C, Kolkhof P, Kim SY, Zannad F. Rationale and design of ARTS: a randomized, double-blind study of BAY

94-8862 in patients with chronic heart failure and mild or moderate chronic kidney disease. *Eur J Heart Fail*. 2012;14:668-675. doi: 10.1093/eurjhf/hfs061

24. Gonzalez-Blazquez R, Somoza B, Gil-Ortega M, Martin Ramos M, Ramiro-Cortijo D, Vega-Martin E, Schulz A, Ruilope LM, Kolkhof P, Kreutz R, et al. Finerenone Attenuates Endothelial Dysfunction and Albuminuria in a Chronic Kidney Disease Model by a Reduction in Oxidative Stress. *Front Pharmacol*. 2018;9:1131. doi: 10.3389/fphar.2018.01131

25. Grune J, Beyhoff N, Smeir E, Chudek R, Blumrich A, Ban Z, Brix S, Betz IR, Schupp M, Foryst-Ludwig A, et al. Selective Mineralocorticoid Receptor Cofactor Modulation as Molecular Basis for Finerenone's Antifibrotic Activity. *Hypertension*. 2018;71:599-608. doi: 10.1161/HYPERTENSIONAHA.117.10360

26. Kolkhof P, Delbeck M, Kretschmer A, Steinke W, Hartmann E, Barfacker L, Eitner F, Albrecht-Kupper B, Schafer S. Finerenone, a novel selective nonsteroidal mineralocorticoid receptor antagonist protects from rat cardiorenal injury. *J Cardiovasc Pharmacol*. 2014;64:69-78. doi: 10.1097/FJC.0000000000000091

27. Lattenist L, Lechner SM, Messaoudi S, Le Mercier A, El Moghrabi S, Prince S, Bobadilla NA, Kolkhof P, Jaisser F, Barrera-Chimal J. Nonsteroidal Mineralocorticoid Receptor Antagonist Finerenone Protects Against Acute Kidney Injury-Mediated Chronic Kidney Disease: Role of Oxidative Stress. *Hypertension*. 2017;69:870-878. doi: 10.1161/HYPERTENSIONAHA.116.08526

28. Chaumais MC, Djessas MRA, Thuillet R, Cumont A, Tu L, Hebert G, Gaignard P, Huertas A, Savale L, Humbert M, et al. Additive protective effects of sacubitril/valsartan and bosentan on vascular remodelling in experimental pulmonary hypertension. *Cardiovasc Res*. 2021;117:1391-1401. doi: 10.1093/cvr/cvaa200

29. Le Menuet D, Isnard R, Bichara M, Viengchareun S, Muffat-Joly M, Walker F, Zennaro MC, Lombes M. Alteration of cardiac and renal functions in transgenic mice overexpressing human mineralocorticoid receptor. *J Biol Chem*. 2001;276:38911-38920. doi: 10.1074/jbc.M103984200

30. Bouvard C, Tu L, Rossi M, Desroches-Castan A, Berrebeh N, Helfer E, Roelants C, Liu H, Ouarne M, Chaumontel N, et al. Different cardiovascular and pulmonary phenotypes for single- and double-knock-out mice deficient in BMP9 and BMP10. *Cardiovasc Res*. 2021. doi: 10.1093/cvr/cvab187

31. Guignabert C, Phan C, Seferian A, Huertas A, Tu L, Thuillet R, Sattler C, Le Hiress M, Tamura Y, Jutant EM, et al. Dasatinib induces lung vascular toxicity and predisposes to pulmonary hypertension. *The Journal of clinical investigation*. 2016;126:3207-3218. doi: 10.1172/JCI86249

32. Tamura Y, Phan C, Tu L, Le Hiress M, Thuillet R, Jutant EM, Fadel E, Savale L, Huertas A, Humbert M, et al. Ectopic upregulation of membrane-bound IL6R drives vascular remodeling in pulmonary arterial hypertension. *The Journal of clinical investigation*. 2018;128:1956-1970. doi: 10.1172/JCI96462

33. Tu L, De Man FS, Girerd B, Huertas A, Chaumais MC, Lecerf F, Francois C, Perros F, Dorfmuller P, Fadel E, et al. A critical role for p130Cas in the progression of pulmonary hypertension in humans and rodents. *Am J Respir Crit Care Med*. 2012;186:666-676. doi: 10.1164/rccm.201202-0309OC

34. Tu L, Desroches-Castan A, Mallet C, Guyon L, Cumont A, Phan C, Robert F, Thuillet R, Bordenave J, Sekine A, et al. Selective BMP-9 Inhibition Partially Protects Against Experimental Pulmonary Hypertension. *Circulation research*. 2019;124:846-855. doi: 10.1161/CIRCRESAHA.118.313356

35. Liao Y, Smyth GK, Shi W. The R package Rsubread is easier, faster, cheaper and better for alignment and quantification of RNA sequencing reads. *Nucleic Acids Res*. 2019;47:e47. doi: 10.1093/nar/gkz114

36. Chen Y, Lun AT, Smyth GK. From reads to genes to pathways: differential expression analysis of RNA-Seq experiments using Rsubread and the edgeR quasi-likelihood pipeline. *F1000Res*. 2016;5:1438. doi: 10.12688/f1000research.8987.2

37. Ritchie ME, Phipson B, Wu D, Hu Y, Law CW, Shi W, Smyth GK. limma powers differential expression analyses for RNA-sequencing and microarray studies. *Nucleic Acids Res*. 2015;43:e47. doi: 10.1093/nar/gkv007

38. Le Vely B, Phan C, Berrebeh N, Thuillet R, Ottaviani M, Chelgham MK, Chaumais MC, Amazit L, Humbert M, Huertas A, et al. Loss of cAbl Tyrosine Kinase in Pulmonary Arterial Hypertension Causes Dysfunction of Vascular Endothelial Cells. *Am J Respir Cell Mol Biol*. 2022. doi: 10.1165/rcmb.2021-0332OC

39. Viengchareun S, Kamenicky P, Teixeira M, Butlen D, Meduri G, Blanchard-Gutton N, Kurschat C, Lanel A, Martinerie L, Sztal-Mazer S, et al. Osmotic stress regulates mineralocorticoid receptor expression in a novel aldosterone-sensitive cortical collecting duct cell line. *Mol Endocrinol*. 2009;23:1948-1962. doi: 10.1210/me.2009-0095

40. Le Billan F, Khan JA, Lamribet K, Viengchareun S, Bouligand J, Fagart J, Lombes M. Cistrome of the aldosterone-activated mineralocorticoid receptor in human renal cells. *FASEB J*. 2015;29:3977-3989. doi: 10.1096/fj.15-274266

41. Kolkhof P, Joseph A, Kintscher U. Nonsteroidal mineralocorticoid receptor antagonism for cardiovascular and renal disorders - New perspectives for combination therapy. *Pharmacol Res*. 2021;172:105859. doi: 10.1016/j.phrs.2021.105859

42. Pitt B, Filippatos G, Agarwal R, Anker SD, Bakris GL, Rossing P, Joseph A, Kolkhof P, Nowack C, Schloemer P, et al. Cardiovascular Events with Finerenone in Kidney Disease and Type 2 Diabetes. *N Engl J Med*. 2021. doi: 10.1056/NEJMoa2110956

43. Bakris GL, Agarwal R, Anker SD, Pitt B, Ruilope LM, Rossing P, Kolkhof P, Nowack C, Schloemer P, Joseph A, et al. Effect of Finerenone on Chronic Kidney Disease Outcomes in Type 2 Diabetes. *N Engl J Med*. 2020;383:2219-2229. doi: 10.1056/NEJMoa2025845

44. Amazit L, Le Billan F, Kolkhof P, Lamribet K, Viengchareun S, Fay MR, Khan JA, Hillisch A, Lombes M, Rafestin-Oblin ME, et al. Finerenone Impedes Aldosterone-dependent Nuclear Import of the Mineralocorticoid Receptor and Prevents Genomic Recruitment of Steroid Receptor Coactivator-1. *J Biol Chem*. 2015;290:21876-21889. doi: 10.1074/jbc.M115.657957

45. Bienvenu LA, Morgan J, Rickard AJ, Tesch GH, Cranston GA, Fletcher EK, Delbridge LM, Young MJ. Macrophage mineralocorticoid receptor signaling plays a key role in aldosterone-independent cardiac fibrosis. *Endocrinology*. 2012;153:3416-3425. doi: 10.1210/en.2011-2098

46. Kuhn E, Bourgeois C, Keo V, Viengchareun S, Muscat A, Meduri G, Le Menuet D, Feve B, Lombes M. Paradoxical resistance to high-fat diet-induced obesity and altered macrophage

polarization in mineralocorticoid receptor-overexpressing mice. *Am J Physiol Endocrinol Metab*. 2014;306:E75-90. doi: 10.1152/ajpendo.00323.2013

FIGURE LEGENDS:

Figure 1. Increased expression of mineralocorticoid receptor (MR) in vascular cells of remodeled pulmonary arteries in lungs of idiopathic PAH patients, monocrotaline (MCT) and sugen+hypoxia (SuHx) rats. (A) Representative photomicrographs of distal pulmonary arteries in lung sections from controls and PAH patients showing overexpression of MR (red color) within pulmonary arterial wall in controls and idiopathic PAH patients and **(B)** in control, MCT, and SuHx rats. Pulmonary artery smooth muscle cells (PA-SMCs) were visualized with an anti-smooth muscle α-actin (α-SMA) antibody (green color). Nuclei were counterstained with DAPI (4',6-diamidino-2-phenylindole; blue color). L: lumen.

Figure 2. Mineralocorticoid receptor (MR) inhibition attenuates proliferation of human pulmonary artery smooth muscle cells (PA-SMCs) derived from PAH patients. (**A**) Hierarchical clustering analysis reveals the differentially expressed genes (DEGs) between transcripts in human PA-SMCs treated with scrambled or MR siRNA with a cutoff of *P*-value < 0.01 and a fold change > 1.5 (n = 4 each group). **(B)** Graph representation of the top 10 enriched terms derived from GO Biological Process, KEGG and Reactome. The blue line indicates with a pFDR < 0.01. **(C)** Volcano plot highlighting significant genes differentially expressed between human PA-SMCs transfected with either a scrambled sequence (src seq) or MR siRNA. Red spots indicate upregulated genes in PA-SMCs transfected with MR siRNA. Blue spots indicate genes downregulated in PA-SMCs transfected with MR siRNA. Genes of the Reactome pathway related to the mitotic cell cycle shown in B are highlighted by boxes. **(D)** Representative photomicrographs of distal pulmonary arteries in lung sections from controls and PAH patients showing the colocalization of MR (red color) with proliferating cell nuclear antigen (PCNA; white color). Nuclei were counterstained with DAPI (4',6-diamidino-2-phenylindole; blue color). **(E)** Proliferative potential of human PA-SMCs cultured with 5% fetal calf serum (FCS) with or without MR inhibition by RNA-interference or **(F)** in presence of finerenone. Horizontal lines display the mean ± SEM. ** *P*-value < 0.01, *** *P*-value < 0.001 *versus* 0% FCS; $^{\#}$ *P*-value < 0.05 *versus* 5% FCS.

Figure 3. Transgenic mice overexpressing mineralocorticoid receptor (MR) exhibit remodeling of pulmonary vessels with increased wall thickness in room air: (A) Echocardiographic analysis of the cardiac output (CO) and ratio of acceleration time (AT) to ejection time (ET) in hMR^+ and wild-type mice. **(B)** Values of right ventricular systolic pressure (RVSP) and right ventricular hypertrophy expressed by the Fulton Index in hMR^+ and wild-type mice. **(C)** Representative images of hematoxylin-eosin (HE) staining and α-smooth muscle (SM)-actin and quantification of the percentage of wall thickness and muscularized distal pulmonary arteries in lungs from hMR^+ and wild-type mice. **(D)** Representative images of KI67, PCNA and quantification of the percentage of KI67-positive cells in the muscularized wall of distal pulmonary arteries and of CD68-positive cells in lungs from hMR^+ and wild-type mice. Scale bar= 50 µm in all sections. Horizontal lines display the mean ± SEM. * *P*-value < 0.05, ** *P*-value < 0.01 versus wild-type (WT) littermates. AT= acceleration time; AU= arbitrary unit; ET= ejection time; LV= left ventricle; ns= non-significant; RV= right ventricle; S= septum.

Figure 4. Chronic treatment with finerenone partially reverses PH in the monocrotaline (MCT) and sugen+hypoxia (SuHx) rat models: (A) Experimental strategies used to test the curative effects of finerenone in the MCT rat model of PH. **(B)** Ratios of acceleration time (AT) to ejection time (ET) obtained by transthoracic echocardiography. **(C)** Values of mean systemic blood pressure (BP)**, (D)** mean pulmonary artery pressure (mPAP), cardiac output (CO), total pulmonary vascular resistance

(TPVR) and right ventricular hypertrophy by the Fulton Index. **(E)** Experimental strategies used to test the curative effects of finerenone in the SuHx rat model of PH. **(F)** Ratios of AT/ET obtained by transthoracic echocardiography. **(G)** Values of mean systemic BP**, (H)** mPAP, CO, TPVR and Fulton Index. * *P*-value < 0.05, *** *P*-value < 0.001, **** *P*-value < 0.0001 vehicle-treated control rats; $^{\#}$ *P*-value < 0.05; $^{\#\#}$ *P*-value < 0.01; $^{\#\#\#\#}$ *P*-value < 0.0001 *versus* MCT or SuHx rats treated with vehicle. AT= acceleration time; AU= arbitrary unit; ET= ejection time; LV= left ventricle; ns= non-significant; RV= right ventricle; S= septum.

Figure 5. Chronic treatment with finerenone attenuates remodeling of both the right ventricle (RV) and pulmonary arteries (PAs) in monocrotaline (MCT) and sugen+hypoxia (SuHx) rats: (A) Representative images and quantifications of picrosirius red staining in the RV myocardium tissues. **(B)** Representative images of hematoxylin-eosin (HE) and α-smooth muscle actin (α-SMA) immunostaining and quantification of the percentage of wall thickness and of muscularized distal PAs in lungs of control, MCT and SuHx rats treated or not with finerenone. Scale bar= 50 µm in all sections. Horizontal lines display the mean ± SEM. *** *P*-value < 0.001; **** *P*-value < 0.0001 *versus* control rats; $^{\#}$ *P*-value < 0.05, $^{\#\#}$ *P*-value < 0.01; $^{\#\#\#}$ *P*-value < 0.001; $^{\#\#\#\#}$ *P*-value < 0.0001 *versus* MCT or SuHx rats treated with vehicle. AU=arbitrary unit.

Figure 6. Chronic treatment with finerenone attenuates inflammatory cell infiltration and vascular cell proliferation in lungs of monocrotaline (MCT) and sugen+hypoxia (SuHx) rats: Representative images and quantifications of the cell proliferation antigen KI67 and CD68 positive cells per pulmonary vessels. Scale bar= 50 µm in all sections. Horizontal lines display the mean ± SEM. ** *P*-value < 0.01; *** *P*-value < 0.001; **** *P*-value < 0.0001 *versus* control rats; $^{\#}$ *P*-value < 0.05; $^{\#\#}$ *P*-value < 0.01; $^{\#\#\#}$ *P*-value < 0.001; $^{\#\#\#\#}$ *P*-value < 0.0001 *versus* MCT or SuHx rats treated with vehicle. AU=arbitrary unit.

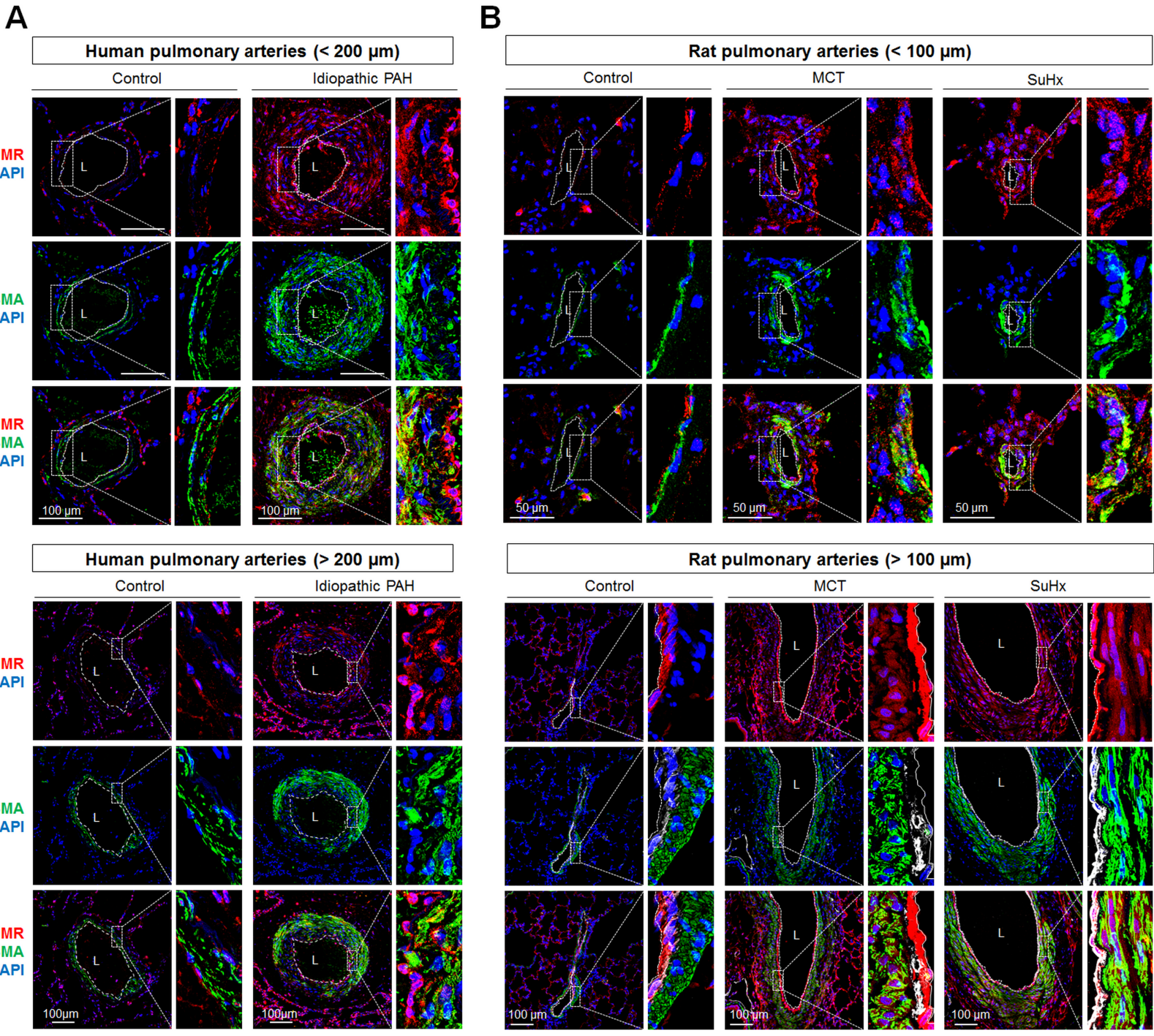
A
Human pulmonary arteries (< 200 μm)
Control
Idiopathic PAH
MR
DAPI
α-SMA
DAPI
MR
α-SMA
DAPI
L
100 μm
Human pulmonary arteries (> 200 μm)
Control
Idiopathic PAH
MR
DAPI
α-SMA
DAPI
MR
α-SMA
DAPI
L
100μm
B
Rat pulmonary arteries (< 100 μm)
Control
MCT
SuHx
L
50 μm
Rat pulmonary arteries (> 100 μm)
Control
MCT
SuHx
L
100 μm

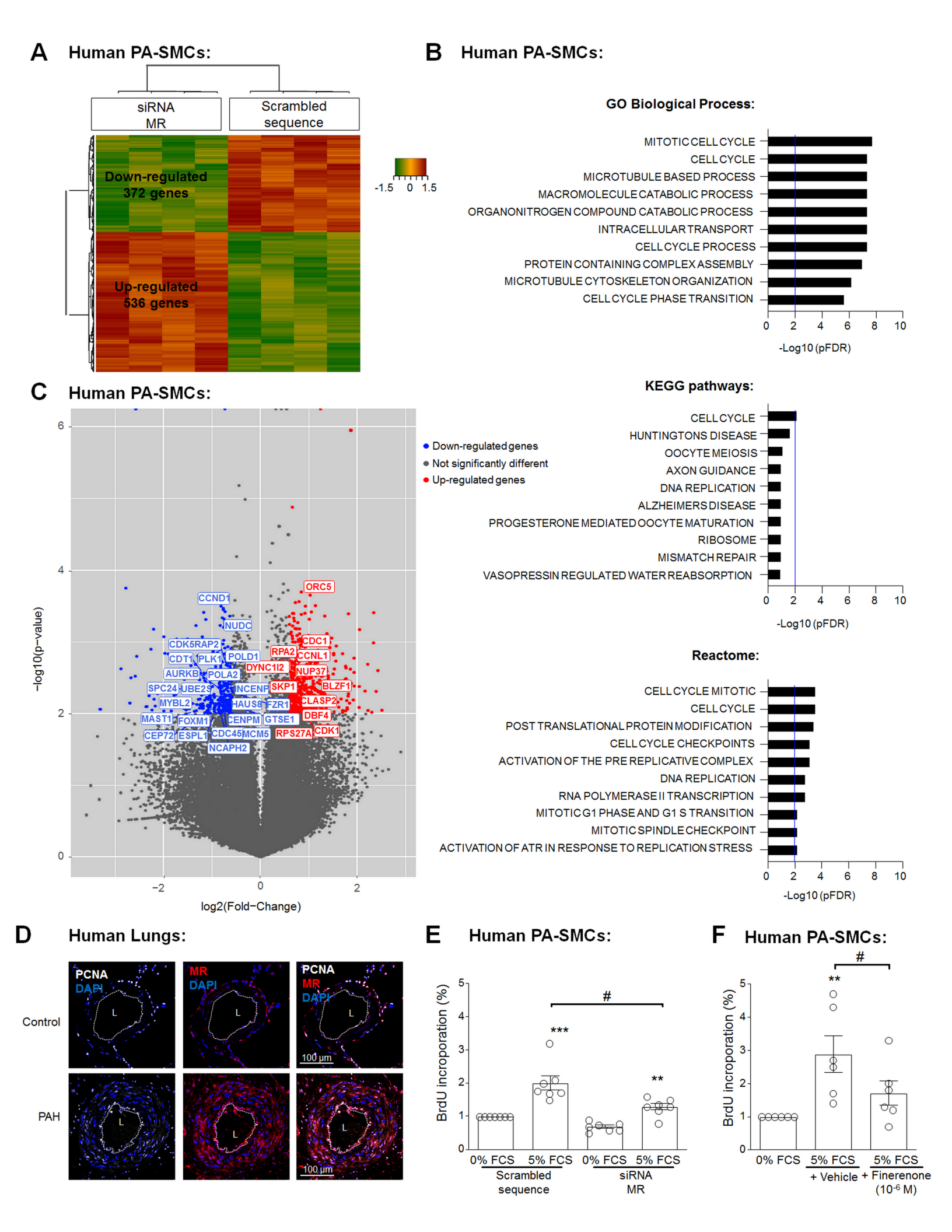
A
Human PA-SMCs:
siRNA MR
Scrambled sequence
Down-regulated 372 genes
Up-regulated 536 genes
-1.5 0 1.5
B
Human PA-SMCs:
GO Biological Process:
MITOTIC CELL CYCLE
CELL CYCLE
MICROTUBULE BASED PROCESS
MACROMOLECULE CATABOLIC PROCESS
ORGANONITROGEN COMPOUND CATABOLIC PROCESS
INTRACELLULAR TRANSPORT
CELL CYCLE PROCESS
PROTEIN CONTAINING COMPLEX ASSEMBLY
MICROTUBULE CYTOSKELETON ORGANIZATION
CELL CYCLE PHASE TRANSITION
0 2 4 6 8 10
-Log10 (pFDR)
C
Human PA-SMCs:
Down-regulated genes
Not significantly different
Up-regulated genes
−log10(p−value)
log2(Fold−Change)
ORC5
CCND1
NUDC
CDC1
CDK5RAP2
RPA2
CDT1
PLK1
POLD1
CCNL1
DYNC1I2
NUP37
AURKB
POLA2
SKP1
BLZF1
SPC24
UBE2S
INCENP
CLASP2
MYBL2
HAUS8
FZR1
DBF4
MAST1
FOXM1
CENPM
GTSE1
CEP72
ESPL1
CDC45
MCM5
RPS27A
CDK1
NCAPH2
KEGG pathways:
CELL CYCLE
HUNTINGTONS DISEASE
OOCYTE MEIOSIS
AXON GUIDANCE
DNA REPLICATION
ALZHEIMERS DISEASE
PROGESTERONE MEDIATED OOCYTE MATURATION
RIBOSOME
MISMATCH REPAIR
VASOPRESSIN REGULATED WATER REABSORPTION
-Log10 (pFDR)
Reactome:
CELL CYCLE MITOTIC
CELL CYCLE
POST TRANSLATIONAL PROTEIN MODIFICATION
CELL CYCLE CHECKPOINTS
ACTIVATION OF THE PRE REPLICATIVE COMPLEX
DNA REPLICATION
RNA POLYMERASE II TRANSCRIPTION
MITOTIC G1 PHASE AND G1 S TRANSITION
MITOTIC SPINDLE CHECKPOINT
ACTIVATION OF ATR IN RESPONSE TO REPLICATION STRESS
-Log10 (pFDR)
D
Human Lungs:
Control
PAH
PCNA
DAPI
MR
DAPI
PCNA
MR
DAPI
L
100 µm
E
Human PA-SMCs:
BrdU incroporation (%)
#
***
**
0% FCS 5% FCS 0% FCS 5% FCS
Scrambled sequence
siRNA MR
F
Human PA-SMCs:
BrdU incroporation (%)
#
**
0% FCS 5% FCS 5% FCS
+ Vehicle + Finerenone (10-6 M)

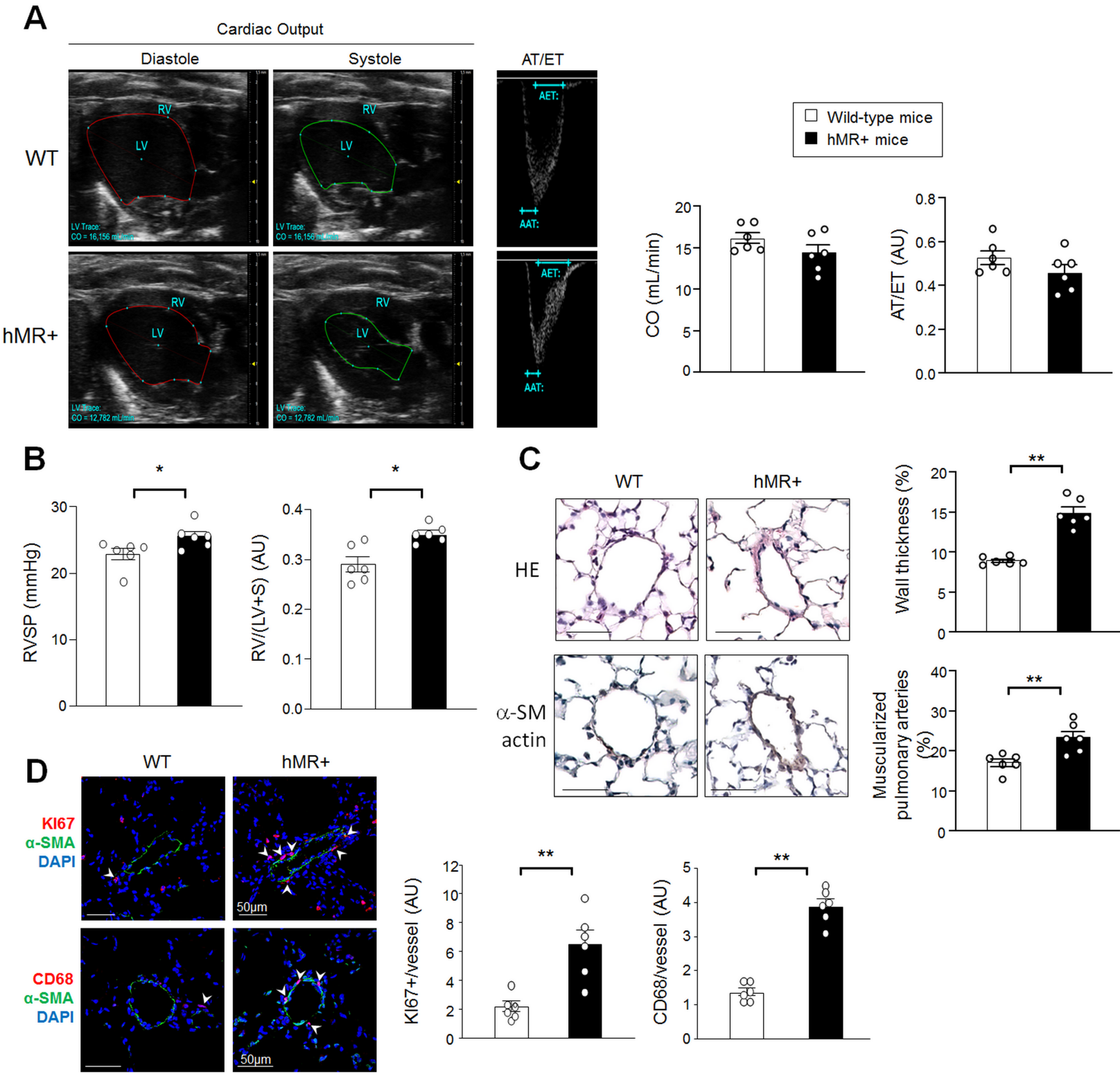
A
Cardiac Output
Diastole
Systole
AT/ET
WT
hMR+
RV
LV
AET:
AAT:
Wild-type mice
hMR+ mice
CO (mL/min)
AT/ET (AU)
B
RVSP (mmHg)
RV/(LV+S) (AU)
C
WT
hMR+
HE
α-SM actin
Wall thickness (%)
Muscularized pulmonary arteries (%)
D
KI67
α-SMA
DAPI
CD68
50μm
KI67+/vessel (AU)
CD68/vessel (AU)

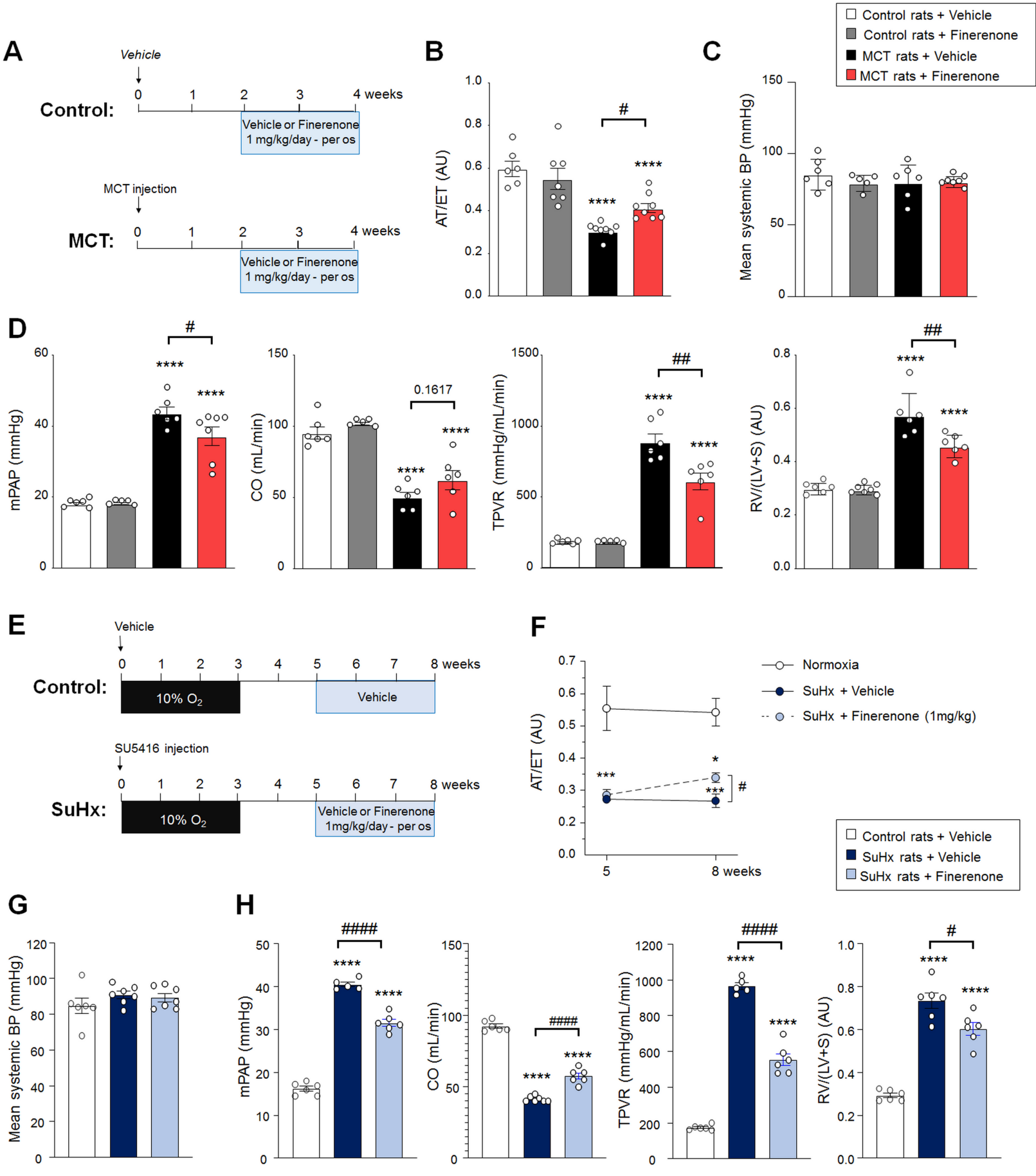
A
Vehicle
Control:
0 1 2 3 4 weeks
Vehicle or Finerenone
1 mg/kg/day - per os
MCT injection
MCT:
0 1 2 3 4 weeks
Vehicle or Finerenone
1 mg/kg/day - per os
B
AT/ET (AU)
#
****
****
C
Mean systemic BP (mmHg)
Control rats + Vehicle
Control rats + Finerenone
MCT rats + Vehicle
MCT rats + Finerenone
D
mPAP (mmHg)
#
****
****
CO (mL/min)
0.1617
****
****
TPVR (mmHg/mL/min)
##
****
****
RV/(LV+S) (AU)
##
****
****
E
Vehicle
Control:
0 1 2 3 4 5 6 7 8 weeks
10% O2
Vehicle
SU5416 injection
SuHx:
0 1 2 3 4 5 6 7 8 weeks
10% O2
Vehicle or Finerenone
1mg/kg/day - per os
F
AT/ET (AU)
Normoxia
SuHx + Vehicle
SuHx + Finerenone (1mg/kg)
***
*
***
#
5
8 weeks
Control rats + Vehicle
SuHx rats + Vehicle
SuHx rats + Finerenone
G
Mean systemic BP (mmHg)
H
mPAP (mmHg)
####
****
****
CO (mL/min)
####
****
****
TPVR (mmHg/mL/min)
####
****
****
RV/(LV+S) (AU)
#
****
****

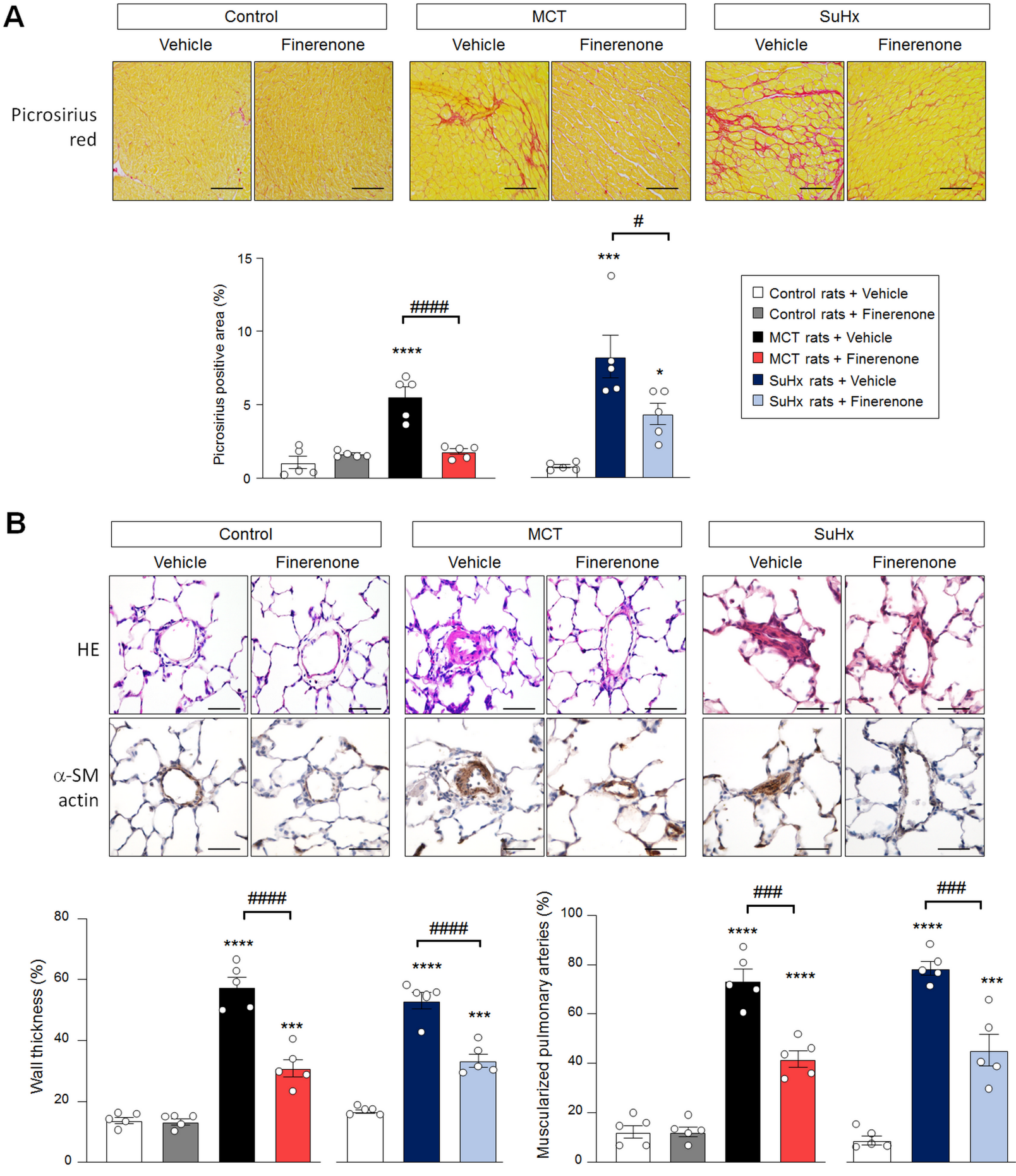
A
Control
MCT
SuHx
Vehicle
Finerenone
Picrosirius red
Picrosirius positive area (%)
15
10
5
0
****
####
***
#
*
Control rats + Vehicle
Control rats + Finerenone
MCT rats + Vehicle
MCT rats + Finerenone
SuHx rats + Vehicle
SuHx rats + Finerenone
B
HE
α-SM actin
Wall thickness (%)
80
60
40
20
0
Muscularized pulmonary arteries (%)
100
80
60
40
20
0
###

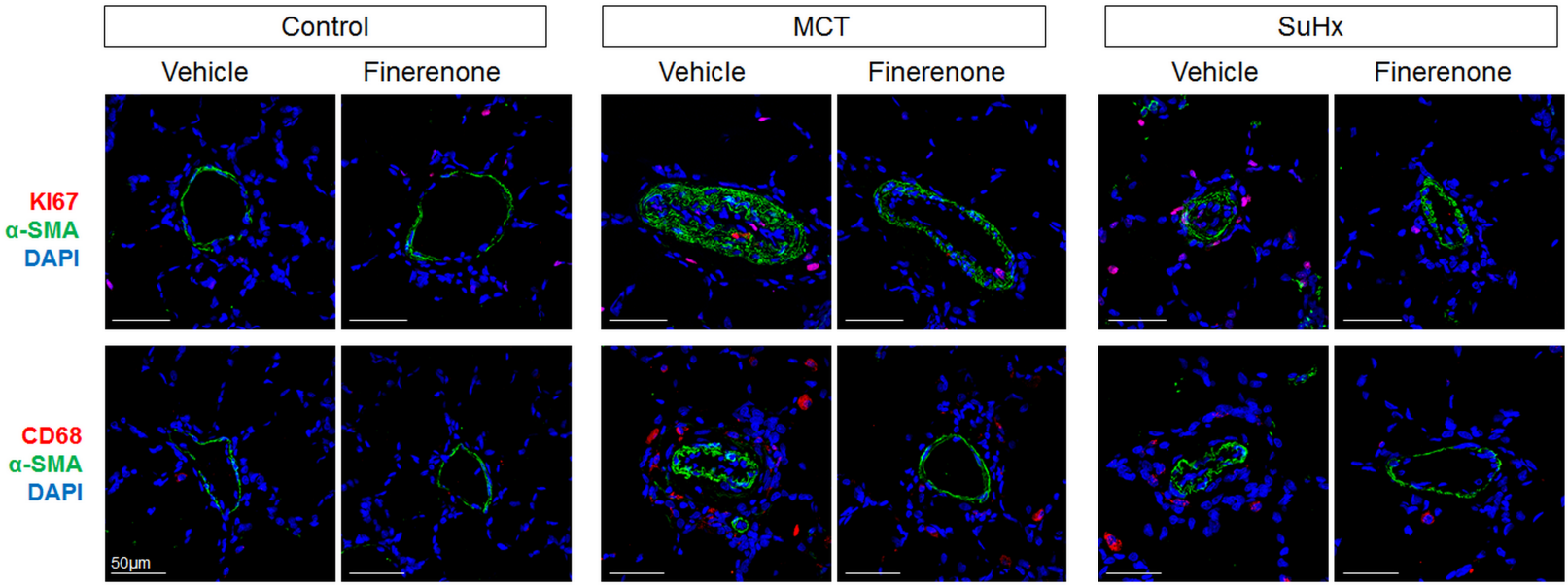
Control
MCT
SuHx
Vehicle
Finerenone
Vehicle
Finerenone
Vehicle
Finerenone
KI67
α-SMA
DAPI
CD68
α-SMA
DAPI
50μm

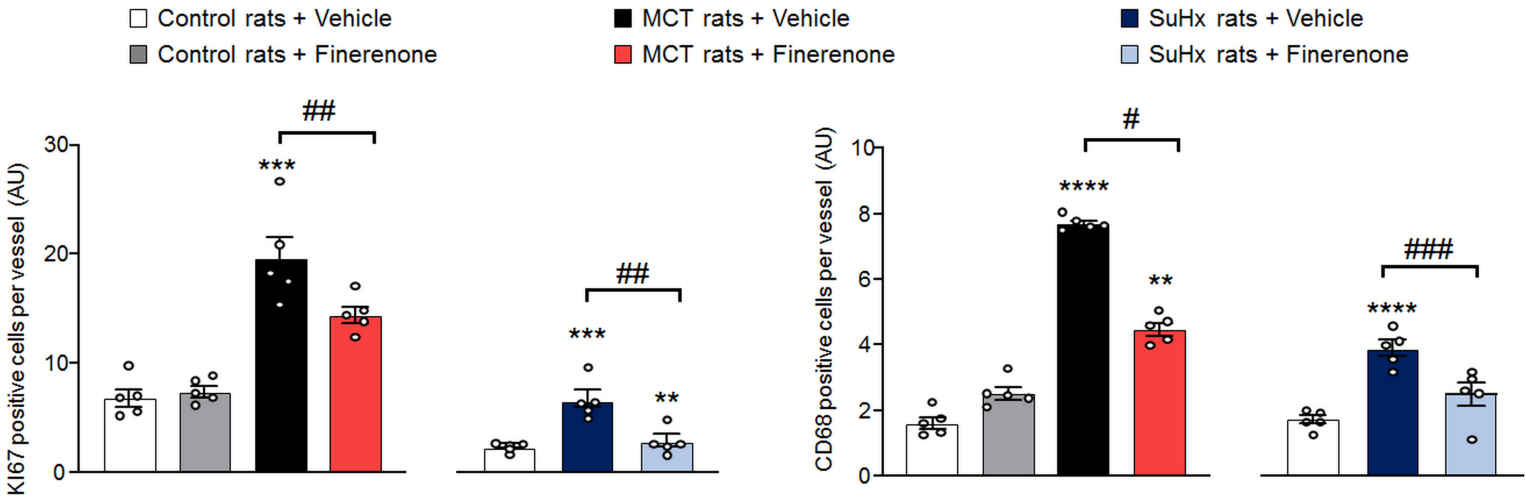
Control rats + Vehicle
Control rats + Finerenone
MCT rats + Vehicle
MCT rats + Finerenone
SuHx rats + Vehicle
SuHx rats + Finerenone
KI67 positive cells per vessel (AU)
CD68 positive cells per vessel (AU)
##
***
##
***
**
#
****
**
##
****
###